

Cite this: *Chem. Sci.*, 2020, 11, 12829 All publication charges for this article have been paid for by the Royal Society of Chemistry

# Dynamic spatial and structural organization in artificial cells regulates signal processing by protein scaffolding†

Bastiaan C. Buddingh',  Antoni Llopis-Lorente,  Loai K. E. A. Abdelmohsen \* and Jan C. M. van Hest \*

Structural and spatial organization are fundamental properties of biological systems that allow cells to regulate a wide range of biochemical processes. This organization is often transient and governed by external cues that initiate dynamic self-assembly processes. The construction of synthetic cell-like materials with similar properties requires the hierarchical and reversible organization of selected functional components on molecular scaffolds to dynamically regulate signaling pathways. The realization of such transient molecular programs in synthetic cells, however, remains underexplored due to the associated complexity of such hierarchical platforms. In this contribution, we effectuate dynamic spatial organization of effector protein subunits in a synthetic biomimetic compartment, a giant unilamellar vesicle (GUV), by associating in a reversible manner two fragments of a split luciferase to the membrane. This induces their structural dimerization, which consequently leads to the activation of enzymatic signaling. Importantly, such organization and activation are dynamic processes, and can be autonomously regulated – thus opening up avenues toward continuous spatiotemporal control over supramolecular organization and signaling in an artificial cell.

Received 17th July 2020  
Accepted 4th November 2020

DOI: 10.1039/d0sc03933k

rsc.li/chemical-science

## Introduction

Versatility and adaptability of biological systems arise from well-defined chemical pathways that control their structural and spatial organizational states. Such states are often dynamic and play a significant role in controlling key biological processes. For example, so-called 'supramolecular organizing centers' (e.g. inflammasomes) are localized higher-order signaling complexes that utilize dynamic protein scaffolding processes to organize downstream operations and integrate upstream signaling events.<sup>1</sup> Enzyme activation by protein dimerization is a particularly powerful concept in such supramolecular regulation – for instance, caspase-1 forms an active heterodimer upon assembly on cytosolic receptors, which initiates an inflammatory cellular response.<sup>1</sup> Inspired by this biochemical logic, scientists from various disciplines have undertaken to mimic such systems and behaviors in synthetic analogs.<sup>2–7</sup> In this regard, self-assembled structures based upon peptides<sup>8,9</sup> or DNA<sup>10–14</sup> have been exemplary in how to program synthetic systems the way biology does; however, these systems

do not display autonomous functionality. Contrary to most synthetic materials, living systems exhibit self-regulating and adaptable behavior that is maintained by dynamic (and transient) processes, where spatiotemporal regulation and organization of the flow of chemical information is critical.<sup>15</sup> Successful programming of dynamic behavior in synthetic materials thus requires implementation of regulatory mechanisms that exert control over the resulting functional ensemble.

In a first approximation, it is possible to identify two general, yet crucial sub-categories to the area of mimicking biological dynamic behavior: (i) the development of synthetic compartmentalized systems that mimic structural aspects of biological entities (*i.e.* cells),<sup>16–20</sup> and (ii) reconstitution of biochemical processes such as protein expression and enzymatic networks to mimic functional aspects of cellular behavior.<sup>21–24</sup> Although either category has been indispensable in building up our knowledge and capacity in this discipline, the merger of these two important properties is required to create cell-like entities that display dynamic behavior. Toward this, our group has previously developed an approach to spatially organize proteins inside a synthetic cell mimic.<sup>25</sup> Although this protein localization process was dynamic, both the structure and function of the protein remained static. Capitalizing on this, we herein demonstrate a self-regulated and dynamic system in which its spatial organization induces a biochemical response inside an artificial cell.

Department of Chemical Engineering and Chemistry, Institute for Complex Molecular Systems, Department of Biomedical Engineering, Eindhoven University of Technology, PO Box 513, 5600 MB Eindhoven, The Netherlands. E-mail: J.C.M.v.Hest@tue.nl; L.K.E.A.Abdelmohsen@tue.nl

† Electronic supplementary information (ESI) available: All experimental details, as well as additional experimental data. See DOI: 10.1039/d0sc03933k







**Fig. 2** Ni-NTA-dependent spatial organization and activation of NanoBiT in GUVs. (a) Bioluminescence micrographs of GUVs loaded with SmBiT and LgBiT (5  $\mu$ M each) that were functionalized with 1% DOGS-NTA-Ni or left unfunctionalized. (b) Bioluminescence of GUVs with or without 2% DOGS-NTA-Ni and varying concentrations of encapsulated LgBiT and SmBiT. The bioluminescence was normalized to the number of GUVs. (c) Bioluminescence micrographs of GUVs loaded with LgBiT (5  $\mu$ M) and either His-SmBiT or NoHis-SmBiT (5  $\mu$ M). The GUVs contained 2% DOGS-NTA-Ni, and sulforhodamine (red) for tracking. Global bioluminescence quantification of corresponding samples is shown in ESI Fig. 8† 2 mM EDTA was added to the external solution and all experiments were performed at pH 7.4.

selective ligands that facilitated the localization of a His-tagged protein to the vesicle membrane through recruitment of its hexahistidine domain.

### Spatio-structural organization controls enzymatic activation

As demonstrated, these His/Ni-NTA interactions are a powerful instrument to induce spatial organization of hierarchical complexes of nanoscopic components inside artificial cells. Yet, recruitment of proteins to the GUV membrane can also promote their structural organization (mediated by dimerization) and – in case of enzymes – subsequent activation, which is a common regulatory process in natural cells. Here, membrane localization increases the local concentration of LgBiT and SmBiT (spatial organization), which is expected to enhance their dimerization (structural organization).

To investigate the enhancement of signaling responses by both spatial and structural organization of the luciferase fragments, the bioluminescence output of populations of vesicles was monitored in bulk measurements, allowing a more quantitative assessment of the overall luciferase reconstitution than that offered by microscopy. To correct for the concentration of vesicles in each sample, the bioluminescence was normalized to

the fluorescence of an inert fluorophore loaded into the GUVs. Indeed, the total bioluminescence of vesicles that contained DOGS-NTA-Ni was markedly higher than that of vesicles without Ni-NTA groups (Fig. 2b). The absolute bioluminescent signal depended on the concentration of both fragments inside the vesicles; the stoichiometry of the interaction was unimportant, but – as expected – higher concentrations of LgBiT and SmBiT produced higher enzymatic activity. At low concentrations of both fragments (0.2 and 1.0  $\mu$ M), the bioluminescent signal in artificial cells without DOGS-NTA-Ni-mediated spatio-structural organization was negligible, whereas organization of the complex at the membrane induced an increase of the signal of up to one order of magnitude. This indicated that membrane recruitment did not only spatially redistribute the enzymatic activity, but also resulted in enhanced activation of signaling. Therefore, spatial organization led to structural organization and enzymatic activation; processes highly resembling protein signaling in biology.

To study if spatial organization of both fragments was required for NanoBiT reconstitution, a SmBiT fragment without His-tag (NoHis-SmBiT) was synthesized, and its ability to form the active complex was evaluated. In a first set of experiments, bioluminescence microscopy was used to assess the relative membrane-to-lumen signal ratio and therefore the spatial localization of the fragments (NanoBiT reconstitution) at the membrane. Micrographs showed that the active luciferase is preferentially formed at the membrane only if both LgBiT and SmBiT are His-tagged (Fig. 2c). The GUVs loaded with His-tagged LgBiT and NoHis-SmBiT showed some spontaneous reconstitution of the active luciferase in the lumen, yet spatial organization of the luciferase at the membrane was not observed; thus indicating that both SmBiT and LgBiT should be His-tagged to induce effective complex assembly at the membrane. This was supported by the global luminescence signal (quantified by bulk bioluminescence spectroscopy and normalized to the signal of encapsulated marker to account for the total number of GUVs in the sample), which was higher when both fragments were His-tagged (due to effective dimerization at the membrane) than for NoHis-SmBiT (ESI Fig. 8†). When the GUVs did not contain Ni-NTA on their membrane, His-SmBiT and NoHis-SmBiT samples showed no notable differences in global bioluminescence (originating from spontaneous complementation in the GUV lumen) (ESI Fig. 8†). This also suggested that the intrinsic LgBiT-SmBiT interactions were not significantly altered by the His-tag, as confirmed in control experiments (ESI Fig. 18†).

Altogether, these results demonstrated that spatial organization of both fragments at the GUV membrane and subsequent dimerization of the two fragments promotes subsequent reconstitution of enzymatic activity through formation of a higher-order signaling complex.

### Reversible organization of protein complexes regulates enzymatic signaling

Having established Ni-NTA-mediated spatial organization of proteins in compartmentalized synthetic cells as a strategy to organize protein dimerization and induce signaling, we sought



to control such processes reversibly. Such an approach aims to mimic the dynamic self-assembly in biology, where reversible organization of responsive elements produces the complex behavior apparent in living systems. To this end, we utilized the non-covalent nature of the His-tag/Ni-NTA interaction to enable reversible formation and dissociation of the luciferase fragments, which, in turn, provides control over the activation of enzymatic signaling. The strength of the His-tag/Ni-NTA interaction can be modulated by tuning the pH of the environment; thus, this offers a general framework to interface the internal luciferase signaling with programmable self-regulating or adaptive processes that modulate the internal pH. The  $pK_a$  of the imidazole side chains in the His-tag is 6.0; consequently, acidification of a neutral solution decidedly weakens the His/Ni-NTA interactions. Therefore, by alternatingly increasing and decreasing the pH the reversibility of the system can be demonstrated.

To test the responsiveness of the system to pH, GUVs were treated with small doses of acid or base, followed by 20 min of incubation and subsequent recording of the resulting enzymatic activity. Complexation between His-tagged proteins and Ni-NTA moieties has been reported to occur in a timescale of seconds.<sup>32</sup> In addition, the relatively high diffusion coefficient of small proteins ( $>200 \mu\text{m}^2 \text{s}^{-1}$ ) should allow their rapid assembly/disassembly from the membrane.<sup>33</sup> To ensure rapid equilibration of the internal and external solutions, the vesicles were incubated with alpha-hemolysin, a self-inserting membrane pore.<sup>31</sup>

At pH 7.4 LgBiT and SmBiT formed the active luciferase at the membrane, as expected (Fig. 3). When the pH was decreased to 5.5 by addition of dilute HCl, the membrane-associated bioluminescence disappeared and a somewhat weaker signal originating from the lumen was observed. Not all GUVs emitted a detectable luminescence; this was attributed to the lower activity of the luciferase at pH 5.5 (a previous report found

a reduction of *ca.* 50% at pH 5.5 as compared to pH 7.5 and we found a similar decrease in bulk LgBiT-SmBiT solutions as shown in ESI Fig. 18†),<sup>28</sup> and possibly partial loss of SmBiT from some vesicles with high  $\alpha$ HL content. Gratifyingly, when the pH was reversed to 7.5 the bioluminescent ring reappeared, which

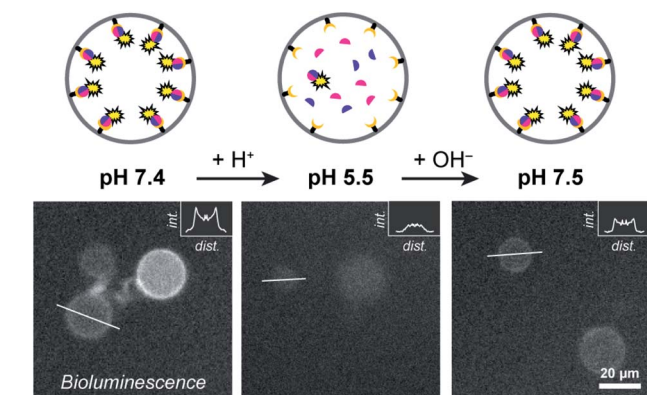


Fig. 3 pH-dependent spatial organization of NanoBiT at the membrane. The bioluminescence of different GUVs was recorded following acidification and subsequent basification of the external solution. GUVs contained DOGS-NTA-Ni (1%), LgBiT and SmBiT ( $5 \mu\text{M}$  each).  $\alpha$ -Hemolysin ( $20 \mu\text{g ml}^{-1}$ ) facilitated equilibration of the pH over the membrane. The insets display the luminescence intensities along a cross section of the GUVs (indicated by white bars). Note the absence of membrane-associated peaks at acidic pH.

Fig. 4 Integrated pre-programmed control over spatio-structural organization and enzymatic signaling of LgBiT and SmBiT in GUVs. (a) Spatial-structural organization and enzymatic signaling of LgBiT and SmBiT ( $5 \mu\text{M}$  each) is promoted at pH 7.5. Addition of HCl dissociated the complex. Next, urea served as an environmental cue to restore enzymatic signaling at the membrane. Fluorescence micrographs of representative GUVs display internal pH (left panels) and bioluminescence micrographs indicate enzymatic signaling (right panels). Scale bars represent  $5 \mu\text{m}$ . (b) The internal pH of  $>40$  GUVs was tracked using a fluorescent ratiometric pH probe (dextran-FITC-TMR). (c) The bioluminescence localization was quantified by comparing the integrated signal at the membrane and inside the lumen ( $n_{\text{GUVs}} = 18$ ).



indicated that both protein fragments had reassociated with the membrane and reconstituted the active luciferase anew. In control experiments, the pH-responsive binding of His-tagged proteins to the Ni-NTA-containing liposomal membrane was confirmed by confocal microscopy using fluorescent tdTomato (ESI Fig. 19†) and by quantifying the global luciferase activity at different pH values (ESI Fig. 20†). Accordingly, pH-controlled reversible switching of the enzyme activity through reversible organization of NanoBiT at the membrane was demonstrated.

### Enzymatic signaling in artificial cells in response to environmental cues

In a final set of experiments, we aimed at integrated pre-programmed autonomous control over such spatio-structural organization processes by incorporating regulatory enzymatic machinery. This, when viewed in the context of dynamic self-assembly, is a step toward emulating organizational processes in a more biomimetic fashion. To this end, urease – an enzyme that converts urea into ammonia, thereby increasing the pH – was integrated into the system. Urea functioned as environmental cue to steer the controlled assembly of the system. A ratiometric pH probe was also incorporated in the GUV lumen, and time-series data showed the possibility to upregulate the pH according to urease and urea concentration (ESI Fig. 21†).

Spatial organization of SmBiT and LgBiT at the liposome membrane was initiated at pH 7.5 (Fig. 4a). Decreasing the pH to 5.5 by addition of HCl led to spontaneous disassembly of the scaffolded luciferase and consequent disappearance of bioluminescence. Upon addition of urea the pH increased and bioluminescence was restored, confirming the successful association of SmBiT and LgBiT at the membrane (Fig. 4a–c). A fraction of vesicles, however, did not recover their enzymatic signaling; this is attributed to content release of some vesicles during the pH switch. In control experiments where urea was not added to the liposomes after they had been treated with HCl, the pH remained low and bioluminescence was not observed. These results confirm that the spatio-structural organization process was controlled by urease, and not an inherent property of the system.

From a broader perspective, although this particular system (reconstitution of luciferase in response to urea) has no apparent utility in biological terms, artificial cells that produce an output signal in response to molecular cues could potentially be used for diverse applications such as sensing and information processing.

## Conclusions

In summary, we have engineered an artificial cell equipped with dynamic spatial and structural organization processes. Spatial organization was achieved by the localization of two fragments of a split luciferase through specific interactions between the hexahistidine domains on the protein fragments and a Ni-NTA moiety in the lipid membrane. This resulted in the fragments' structural dimerization, and subsequent functional signaling response. Due to the non-covalent, dynamic nature of these

interactions, the supramolecular complex could be reversibly assembled and disassembled. Importantly, the signaling process was controlled by an enzymatic program in response to environmental cues. Our work thus constitutes a significant advancement in the creation of synthetic cell models that approach natural systems in terms of functional complexity.

## Conflicts of interest

There are no conflicts to declare.

## Acknowledgements

Anniek den Hamer and Lenne Lemmens are thanked for providing the LgBiT fragment. Ardjan van der Linden and Pascal Pieters are acknowledged for microscopy support. The Dutch Ministry of Education, Culture and Science (Gravitation program 024.001.035) and the ERC Advanced grant Artisym 694120 are acknowledged for funding.

## References

- 1 J. C. Kagan, V. G. Magupalli and H. Wu, *Nat. Rev. Immunol.*, 2014, **14**, 821–826.
- 2 S. Loescher and A. Walther, *Angew. Chem., Int. Ed.*, 2020, **59**, 5515–5520.
- 3 C. Love, J. Steinkühler, D. T. Gonzales, N. Yandrapalli, T. Robinson, R. Dimova and T. Y. D. Tang, *Angew. Chem., Int. Ed.*, 2020, **59**, 5950–5957.
- 4 H. Zhao, V. Ibrahimova, E. Garanger and S. Lecommandoux, *Angew. Chem., Int. Ed.*, 2020, **59**, 11028–11036.
- 5 V. Mukwaya, P. Zhang, H. Guo, A. Y. Dang-i, Q. Hu, M. Li, S. Mann and H. Dou, *ACS Nano*, 2020, **14**, 7899–7910.
- 6 E. Magdalena Estirado, A. F. Mason, M. Á. Alemán García, J. C. M. van Hest and L. Brunsveld, *J. Am. Chem. Soc.*, 2020, **142**, 9106–9111.
- 7 M. G. F. Last, S. Deshpande and C. Dekker, *ACS Nano*, 2020, **14**, 4487–4498.
- 8 H. Cui, M. J. Webber and S. I. Stupp, *Biopolymers*, 2010, **94**, 1–18.
- 9 E. F. Banwell, E. S. Abelardo, D. J. Adams, M. A. Birchall, A. Corrigan, A. M. Donald, M. Kirkland, L. C. Serpell, M. F. Butler and D. N. Woolfson, *Nat. Mater.*, 2009, **8**, 596–600.
- 10 S. M. Douglas, H. Dietz, T. Liedl, B. Högberg, F. Graf and W. M. Shih, *Nature*, 2009, **459**, 414–418.
- 11 N. C. Seeman and H. F. Sleiman, *Nat. Rev. Mater.*, 2018, **3**, 17068.
- 12 E. Winfree, F. Liu, L. A. Wenzler and N. C. Seeman, *Nature*, 1998, **394**, 539–544.
- 13 P. W. K. Rothmund, *Nature*, 2006, **440**, 297–302.
- 14 B. J. H. M. Rosier, A. J. Markvoort, B. Gumí Audenis, J. A. L. Roodhuizen, A. den Hamer, L. Brunsveld and T. F. A. de Greef, *Nat. Catal.*, 2020, **3**, 295–306.
- 15 T. Pawson, *Science*, 2003, **300**, 445–452.



- 16 R. J. R. W. Peters, M. Marguet, S. Marais, M. W. Fraaije, J. C. M. van Hest and S. Lecommandoux, *Angew. Chem., Int. Ed.*, 2014, **53**, 146–150.
- 17 A. F. Mason, N. A. Yewdall, P. L. W. Welzen, J. Shao, M. van Stevendaal, J. C. M. van Hest, D. S. Williams and L. K. E. A. Abdelmohsen, *ACS Cent. Sci.*, 2019, **5**, 1360–1365.
- 18 S. Deshpande, F. Brandenburg, A. Lau, M. G. F. Last, W. K. Spoelstra, L. Reese, S. Wunnavu, M. Dogterom and C. Dekker, *Nat. Commun.*, 2019, **10**, 1800.
- 19 T. Trantidou, M. Friddin, Y. Elani, N. J. Brooks, R. V. Law, J. M. Seddon and O. Ces, *ACS Nano*, 2017, **11**, 6549–6565.
- 20 R. J. Brea, A. K. Rudd and N. K. Devaraj, *Proc. Natl. Acad. Sci. U. S. A.*, 2016, **113**, 8589–8594.
- 21 V. Noireaux and A. Libchaber, *Proc. Natl. Acad. Sci. U. S. A.*, 2004, **101**, 17669–17674.
- 22 A. M. Tayar, E. Karzbrun, V. Noireaux and R. H. Bar-Ziv, *Proc. Natl. Acad. Sci. U. S. A.*, 2017, **114**, 11609–11614.
- 23 S. N. Semenov, A. S. Y. Wong, R. M. van der Made, S. G. J. Postma, J. Groen, H. W. H. van Roekel, T. F. A. de Greef and W. T. S. Huck, *Nat. Chem.*, 2015, **7**, 160–165.
- 24 J. W. Sadownik, E. Mattia, P. Nowak and S. Otto, *Nat. Chem.*, 2016, **8**, 1–6.
- 25 R. J. R. W. Peters, M. Nijemeisland and J. C. M. van Hest, *Angew. Chem., Int. Ed.*, 2015, **54**, 9614–9617.
- 26 J. A. Bornhorst and J. J. Falke, *Methods Enzymol.*, 2000, **326**, 245–254.
- 27 S. Knecht, D. Ricklin, A. N. Eberle and B. Ernst, *J. Mol. Recognit.*, 2009, **22**, 270–279.
- 28 M. P. Hall, J. Unch, B. F. Binkowski, M. P. Valley, B. L. Butler, M. G. Wood, P. Otto, K. Zimmerman, G. Vidugiris, T. Machleidt, M. B. Robers, H. A. Benink, C. T. Eggers, M. R. Slater, P. L. Meisenheimer, D. H. Klaubert, F. Fan, L. P. Encell and K. V. Wood, *ACS Chem. Biol.*, 2012, **7**, 1848–1857.
- 29 A. S. Dixon, M. K. Schwinn, M. P. Hall, K. Zimmerman, P. Otto, T. H. Lubben, B. L. Butler, B. F. Binkowski, T. Machleidt, T. A. Kirkland, M. G. Wood, C. T. Eggers, L. P. Encell and K. V. Wood, *ACS Chem. Biol.*, 2016, **11**, 400–408.
- 30 S. Pautot, B. J. Frisken and D. A. Weitz, *Langmuir*, 2003, **19**, 2870–2879.
- 31 L. Song, M. R. Hobaugh, C. Shustak, S. Cheley, H. Bayley and J. E. Gouaux, *Science*, 1996, **274**, 1859–1865.
- 32 G. Raghunath and R. B. Dyer, *Langmuir*, 2019, **35**, 12550–12561.
- 33 J. F. Torres, A. Komiya, J. Okajima and S. Maruyama, *Defect Diffus. Forum*, 2012, **326**, 452–458.

